Applied Energy 204 (2017) 702–714

Contents lists available at ScienceDirect

Applied Energy

journal homepage: www.elsevier.com/locate/apenergy

Biodiesel production from high acid value oils with a highly active and stable bifunctional magnetic acid

Yi-Tong Wang [a,c], Zhen Fang [b,*], Xing-Xia Yang [a,c]

[a] Key Laboratory of Tropical Plant Resources and Sustainable Use, Xishuangbanna Tropical Botanical Garden, Chinese Academy of Sciences, 88 Xuefulu, Kunming, Yunnan Province 650223, China
[b] Biomass Group, College of Engineering, Nanjing Agricultural University, 40 Dianjiangtai Road, Nanjing, Jiangsu 210031, China
[c] University of Chinese Academy of Sciences, 19A Yuquan Road, Beijing 100049, China

HIGHLIGHTS

- Bifunctional magnetic catalyst with Bronsted and Lewis sites was synthesized.
- It had high acid content (8.84 mmol/g) and magnetism with 97% biodiesel yield.
- 10 cycles with biodiesel yield > 90% from oleic acid at 90 °C for 4 h reaction.
- >95% biodiesel yield for transesterification of soybean oil was achieved.
- It pretreated high acid value *Jatropha* oil with 5 cycles (AV ≤ 1.64 mg KOH/g).

GRAPHICAL ABSTRACT

Carbonaceous bifunctional magnetic solid acid catalyst with high acid content was synthesized by four-step method: (i) metal (Fe) ion chelation, (ii) calcination, (iii) metal (Zr) ion chelation and embedding, and (iv) sulfonation. It efficiently catalyzed the esterification of oleic acid, transesterification of soybean oil and pretreatment of *Jatropha* oil with easy separation for 10 cycles and high stability.

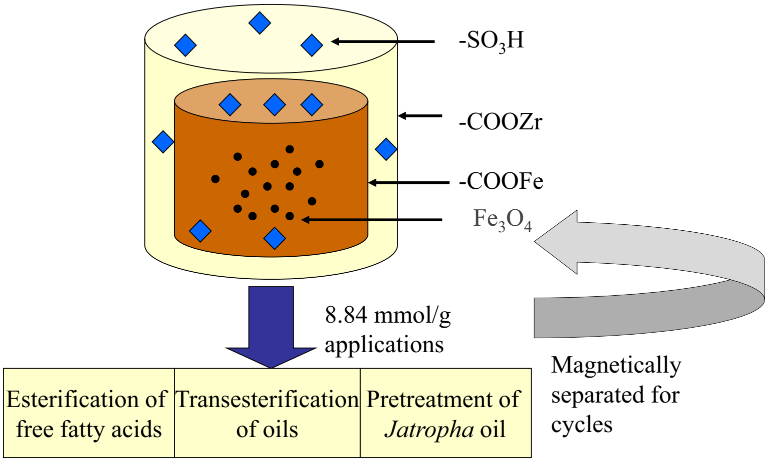

ARTICLE INFO

Article history:
Received 21 April 2017
Received in revised form 3 July 2017
Accepted 15 July 2017

Keywords:
Biodiesel
Pretreatment

ABSTRACT

Biodiesel production was catalyzed by a novel magnetic carbonaceous acid (Zr-CMC-SO_3H@3Fe-C_{400}) with both Brønsted and Lewis sites synthesized by a four-step method: (i) metal (Fe) ion chelation, (ii) calcination, (iii) metal (Zr) ion chelation and embedding, and (iv) sulfonation. It catalyzed the esterification of oleic acid with 97% biodiesel yield, transesterification of high acid value (AV) soybean oil with 95% biodiesel yield, and pretreatment of *Jatropha* oil with AV reduced from 17.2 to 0.7 mg KOH/g. Biodiesel yields (>90%) at 90 °C for 4 h reaction time were obtained for ten cycles by easy magnetic separation which showed potential practical applications in the field of green production. The synthesized catalyst

---

* Corresponding author.
E-mail address: zhenfang@njau.edu.cn (Z. Fang).
URL: http://biomass-group.njau.edu.cn/ (Z. Fang).

http://dx.doi.org/10.1016/j.apenergy.2017.07.060

Jatropha oil
Soybean oil
Magnetic bifunctional acidic catalyst

was characterized with elemental analysis, XRD, ICP-OES, FT-IR, BET, VSM, SEM-EDX, HRTEM, TG-DSC and Boehm titration.

1. Introduction

Along with the expanding urbanization and increasing population in recent years [1], researches on biofuels [such as biodiesel (fatty acid methyl esters; FAMEs), bioethanol and biogas] [2] have attracted more and more attentions from all around the world [3], such as European Union, United States, Malaysia, Indonesia, China and Brazil. While the increasingly serious environmental problems caused by the burning of fossil fuels [4–6], such as global warming, smog [4], decrease of biodiversity and so on [7,8], also make the development of biofuels imminent. Biodiesel [9,10] is regarded as ideal replacement for petroleum diesel because of its renewability, easy storage [11], biodegradability, local availability and environmental friendliness. Compared with conventional diesel, using pure biodiesel can reduce 70% hydrocarbons and 50% particulate matters on exhaust emissions [United States Environmental Protection Agency (US EPA)] [12], and net 78% CO_2 emissions because of its lifecycle [13]. As well as its high O_2 concentration leads to negligible sulfur and aromatics contents that can contribute to emission decrease of SO_2 and unburned hydrocarbons [14,15]. In addition, researchers found biodiesel can be used alone or in different blends without modification in engines [1,16], which reduces a lot of troubles for its applications. Biodiesel production from edible or non-edible oils such as soybean oil [17], waste frying oil [18], cotton seed oil [19], algae oil [20], *Jatropha* oil [21] and microbial lipids [22] catalyzed with homogeneous catalysts by esterification and transesterification process could cause a series of environmental pollution problems coming from product separation and wastewater treatment. But heterogeneous catalysts including solid acids and bases are widely studied in order to replace homogeneous ones. Biodiesel production catalyzed by solid base catalysts requires raw oils having low content of free fatty acids (FFAs) to avoid saponification [23], whereas the process catalyzed by solid acid catalysts such as lignin-derived solid acids [24] has no limit for acid value (AV) in crude oils. Solid acids not only can pretreat raw oils with high AV by esterification reaction but also produce biodiesel by one-step process without saponification phenomenon. So, more and more studies are concentrated on the production of biodiesel by heterogeneous acid catalysts. The surface acid contents of solid acids usually decide their catalytic activities, increasing acid sites including both Lewis and Brønsted acid sites in catalysts would provide more chances for biodiesel production under mild conditions. Reported carbonaceous solid catalysts with both Brønsted and Lewis sites (1.2 mmol/g acid content) were effective to produce furfurals [25]. But, few reports are found for their applications in catalyzing oils with high AV via esterification and transesterification to produce biodiesel. Moreover, in order to cut down energy-consuming and cost of the separation of products and catalysts by centrifugation [26], magnetizing solid catalysts (such as $Fe_3O_4@C\text{-}SO_3H$ [27]) is found to be a cost-effective way because they can be easily separated by a magnet or electromagnetic field with high recovery rate [28]. Currently, little work about bifunctional magnetic solid acid catalysts with both Lewis and Brønsted acid sites for biodiesel production is reported because the balance of the magnetism and activity of the catalyst is very difficult to control. So, new catalyst synthesis methods and suitable materials are very required to develop.

This work aims to directly produce biodiesel or pretreat raw oils with high AV by synthesizing magnetic solid acid catalysts with high acidity and strong magnetism through loading both Lewis and Brønsted acid sites, as well as magnetic particles in a carbonaceous support. Reaction variables were optimized for biodiesel production by single-factor and orthogonal experiments. Catalysts before and after reaction were characterized by various analytic techniques.

2. Experimental

2.1. Materials

Sodium carboxymethylcellulose (CMC) powders with viscosity of 300–800 mPa s were bought from Sinopharm Chemical Reagent Co., Ltd. (Shanghai). Analytical reagents of dehydrated methanol ($\geq$99.5%), dichloromethane ($\geq$99.0%), H_2SO_4 ($\geq$98.0%), NaOH ($\geq$96%), oleic acid (about 80% purity with other fatty acids) and HCl ($\geq$36.0–38.0%) were purchased from Xilong Chemical Factory Co., Ltd. (Shantou, Guangdong). $Fe_2(SO_4)_3$ ($\geq$99.7%) with 21–23% Fe, $ZrOCl_2{\cdot}8H_2O$ ($\geq$98.0%) and Fe_3O_4 nanoparticles ($\geq$99.5%, 20 nm) were from Aladdin Industrial Co., Ltd. (Shanghai). Phenolphthalein, bromocresol green, methyl red and anhydrous sodium carbonate ($\geq$99.9%) were from Tianjin chemical reagent research institute (Tianjin). Fe micro particles ($\geq$98%, 75–425 μm) were purchased from Tianjin recovery technology development Co., Ltd (Tianjin). Seven methyl esters [heptadecanoic acid ($C_{17:0}$), palmitate ($C_{16:0}$), linolenate ($C_{16:1}$), stearate ($C_{18:0}$), oleate ($C_{18:1}$), linoleate ($C_{18:2}$) and linolenate ($C_{18:3}$)] ($\geq$99.0%) were from Sigma (Shanghai) as standards for chromatographic analysis. Soybean oil with AV of 0.7 mg KOH/g and molecular weight (MW) of 881.2 g/mol was bought from a Carrefour supermarket (Kunming, Yunnan), which was blended with oleic acid to achieve different AVs of 42.41, 82.94 and 123.48 mg KOH/g and corresponding MWs of 843.84, 828.48 and 827.30 g/mol for experiments. *Jatropha* oil (AV of 17.2 mg KOH/g and MW of 860.0 g/mol) was obtained from Xishuangbanna Tropical Botanical Garden (Menlun, Yunnan). Deionized water was produced in a water purification system (electrical conductivity was 18.2 MΩ cm, Milli-Q Academic, Merck Millipore, Darmstadt, Germany).

2.2. Catalyst preparation

2.2.1. Preparation of Fe-C_T particles

In Scheme 1-i, carbonaceous Fe-C_T particles were synthesized as magnetic core. About 200 mL CMC solution with concentration of 20 g/L was added dropwise into 200 mL $Fe_2(SO_4)_3$ solution (1 mol/L) to yield precipitate (CMC-COOFe) by metal (Fe) ion chelation reaction under magnetic stirring at room temperature for 3 h. The precipitate was filtered (pore size of 1–3 μm), washed with deionized water until *pH* reaching about 7, dried at 105 °C (WFO-710, EYELA, Tokyo Rikakikai Co., Ltd.) overnight, and ground (particle size <425 μm). The obtained particles (10 g) were added into 50 mL $Fe_2(SO_4)_3$ solution (0.1 mol/L) at room temperature for 3 h to homogeneously load Fe ion further, then washed and dried according to the steps described above. The solid particles were further calcined at 300–600 °C with heating rate of 1 °C/min in a tubular furnace (SGL-1100, Shanghai Daheng Optics and Fine Mechanics Co., Ltd.) under inert nitrogen flowing (200 mL/min), for 2 h (excluding heating and cooling time) to be magnetized (Fe^{3+} was reduced by C to Fe_3O_4 magnetic particles). The resulted

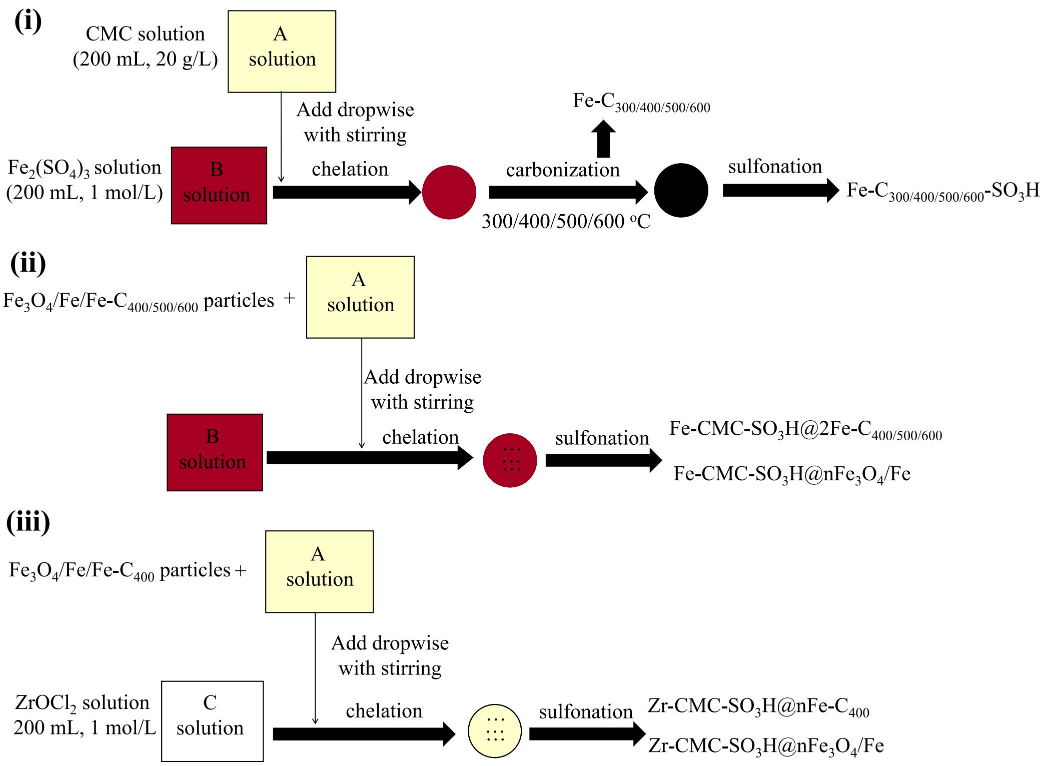

Scheme 1. Workflow of catalyst preparation.

magnetic carbonaceous particles (Fig. 1a) were named as Fe-C$_T$ (Subscript T is calcination temperature: 300/400/500/600 °C).

2.2.2. Synthesis of magnetic Fe-C$_T$-SO$_3$H acid

In Scheme 1-i, the magnetic carbonaceous particles were further sulfonated to solid acids. Magnetic carbonaceous Fe-C$_T$ particles (5 g) and 100 mL H$_2$SO$_4$ with concentration of 98% were added into a high temperature resistant serum bottle (150 mL). The bottle was heated at 150 °C in oil bath (HH-SJ4CD, Jintan city Youlian Instrument Research Institute, Zhejiang) with magnetic stirring for 16 h sulfonation for loading sulfonic acid groups. After reaction and cooling, the mixture including hot sulfuric acid and activated catalyst in the bottle was transferred to a 500 mL flask with deionized water, the particles were filtered (pore size of

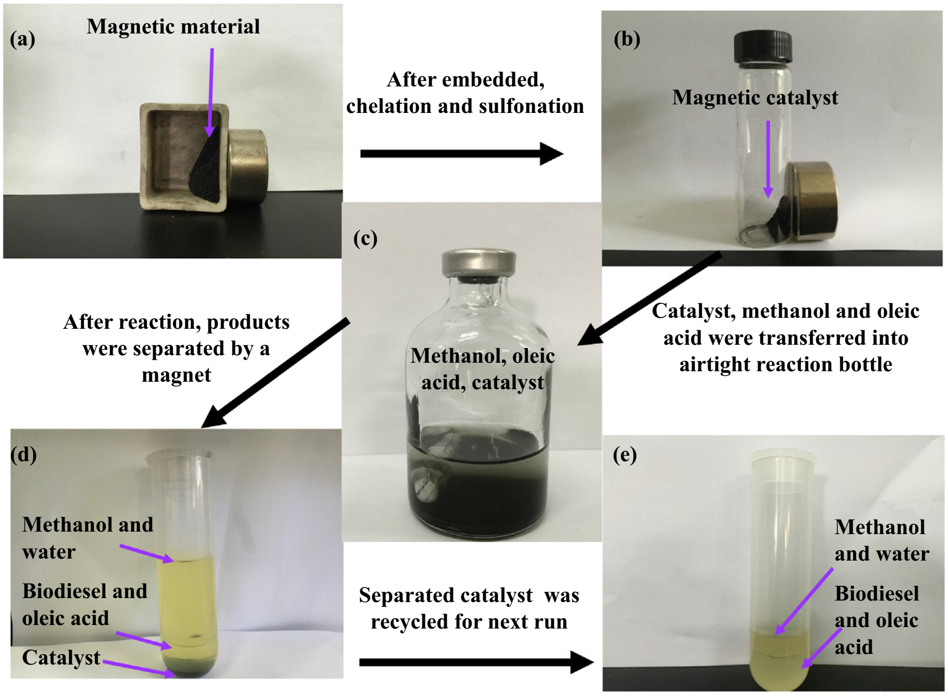

Fig. 1. Biodiesel production from oleic acid esterification and products separation.

0.45 μm), washed with hot water (≥80 °C) until *pH* reaching about 7, and dried in a freeze dryer (PDU-1200, EYELA, Tokyo Rikakikai Co., Ltd.) at −47 °C until complete dry. The sulfonated particles were ground to <75 μm, and named as Fe-C_T-SO_3H catalyst.

2.2.3. Preparation of Fe-CMC-SO_3H@2Fe-C_T and Zr-CMC-SO_3H@nFe-C_T catalysts

Since magnetic carbonaceous Fe-C_T particles cannot provide enough places for linking sulfonic acid groups and easily dissolve, they were re-coated with CMC in order to protect the magnetic core (Fe_3O_4) from dissolution in sulfuric acid and provide enough surface to load both Lewis (CMC-COOZr or CMC-COOFe) and Brønsted (—SO_3H) acid sites. In Scheme 1-ii, Fe-$C_{400/500/600}$ particles (2 g) were mixed and suspended in 200 mL CMC solution (20 g/L), and the mixture was added dropwise into $Fe_2(SO_4)_3$ solution (1 mol/L, 200 mL) with magnetic stirring at room temperature for 3 h to yield precipitate by Fe ion chelation. The precipitate was filtered (pore size of 1–3 μm), washed with deionized water and dried at 105 °C overnight. The dried precipitate was sulfonated, filtered, washed, freeze dried, ground and named as Fe-CMC-SO_3H@2Fe-C_T [2 (g) is the weight of Fe-C_T, it can be changed to n (g)]. In Scheme 1-iii, similar procedure was conducted for the preparation of Zr-CMC-SO_3H@nFe-C_{400}, while $Fe_2(SO_4)_3$ solution was replaced by 200 mL $ZrOCl_2$ solution (1 mol/L), and the dosage of Fe-C_{400} particles could be n (g) (n = 1, 2 or 3). The synthesized catalysts were named as Zr-CMC-SO_3H@nFe-C_T (Subscript T is calcination temperature of Fe-C_T, and n is the weight of Fe-C particles added in CMC solution).

2.2.4. Preparation of Fe-CMC-SO_3H@nFe_3O_4, Fe-CMC-SO_3H@nFe, Zr-CMC-SO_3H@nFe_3O_4 and Zr -CMC-SO_3H@nFe catalysts

Instead of using the synthesized Fe-C_T particles as magnetic core, commercial inexpensive magnetic micro-Fe or nano-Fe_3O_4 particles were directly coated with CMC to load the acid sites. For the preparation of Fe-CMC-SO_3H@nFe_3O_4 (Scheme 1-ii), different weights of Fe_3O_4 nanoparticles were mixed with 200 mL CMC solution (20 g/L), and the mixture was added dropwise into $Fe_2(SO_4)_3$ solution (1 mol/L, 200 mL) at room temperature for 3 h to yield precipitate (Fe_3O_4 particles coated by CMC-COOFe). The obtained precipitate was filtered (pore size of 1–3 μm), washed with deionized water and dried at 105 °C overnight. The dried particles were directly sulfonated without calcination. Similarly, other catalysts were synthesized by replacing Fe_3O_4 particles with Fe microparticles for the preparation of Fe-CMC-SO_3H@nFe, and replacing $Fe_2(SO_4)_3$ solution with 200 mL $ZrOCl_2$ solution (1 mol/L) for the preparation of Zr-CMC-SO_3H@nFe_3O_4 and Zr-CMC-SO_3H@nFe (Scheme 1-iii). After sulfonated, the synthesized catalysts were named as Fe-CMC-SO_3H@nFe_3O_4, Fe-CMC-SO_3H@nFe, Zr-CMC-SO_3H@nFe_3O_4 and Zr-CMC-SO_3H@nFe, respectively (where n is the weight of added Fe_3O_4 or Fe particles, with values of 0.5, 1, 1.5, 2, 3, 5, 7 and 9 g for Fe_3O_4, and 5, 7 and 9 g for Fe).

2.3. Catalyst characterization

The carbonaceous magnetic carriers of Fe-C_T and sulfonated catalysts were analyzed by many techniques. The contents of Fe and Zr in catalysts were measured by inductively coupled plasma-optical emission spectrometer (ICP-OES) after calcined and dissolved in concentrated acid solution (Optima 5300, PerkinElmer Inc, Waltham, MA), and the contents of Fe, C, O and S (H is undetectable and excluded) on surface were detected by energy dispersive X-ray spectroscopy (EDX; Quanta 200, FEI, Hillsboro, OR). Elemental compositions (C, H, N, S) in catalysts were determined by an element analyzer (Vario EL III CHONS, Elementar Analysensysteme GmbH, Hanau, Germany). X-ray diffraction (XRD) diffractometer (Rigaku Rotaflex RAD-C, Tokyo) with CuKα radiation (40 kv and 200 mA) was used to detect the crystalline phases (by comparing with the cards from Joint Committee on Powder Diffraction Standards, JCPDS: 04-0850, 16-0818). Vibrating sample magnetometer (VSM) (lakeshore7407, Lake Shore Cryotronics, Inc., Westerville, OH) was applied for the magnetism measurement. Fourier transform-infrared (FT-IR; from 450 to 4000 cm^{-1} with a resolution of 4 cm^{-1}, with the standard KBr disc method) spectra were recorded on Nicolet *is*10 spectroscopy (Thermo Fisher Scientific Co. Ltd., Waltham, MA). Thermogravimetric analysis - differential scanning calorimetry (TG-DSC) analysis from room temperature to 1000 °C with heating rate of 5 °C/min was conducted on STA449F3 (NETZSCH-Gerätebau GmbH, Selb, Germany). Surface area and pore volume were analyzed by Tristar II 3020 (Micromeritics Instrument Co., Ltd., Northcross, GA) with N_2 adsorption, using Bruner Emmett and Teller (BET) method. Scanning electron microscope (SEM) was applied for the analysis of the morphologies (Quanta 200, FEI, Hillsboro, OR). High resolution-transmission electronic microscope (HRTEM) with Energy dispersion X-ray spectrum (EDX) was used for analyzing the nanostructures of the catalyst (FEI TECNAI G2 F30S-TWIN STEM, Hillsboro, OR). Acid contents over catalysts surface were determined by Boehm titration method with NaOH [29]. Catalyst (about 0.1 g) was mixed with 50 mL 17 mmol/L NaOH solution in a flask, sonicated in an ultrasonic cleaner to neutralize surface acidity for 12 h. The suspension was filtered by 0.22 μm filter membrane to remove catalyst. HCl solution (22 mmol/L, 15 mL) was added into 10 mL filtrate, and excessive HCl was back-titrated by NaOH solution using phenolphthalein as indicator [29].

2.4. Biodiesel production and analysis

Biodiesel was produced from oleic acid or the blended soybean oil with high AV catalyzed by synthesized magnetic solid acids. For the esterification of oleic acid (Fig. 1), oleic acid (about 2.82 g), dehydrated methanol (with methanol to oil molar ratio of 6/1–20/1) and catalyst (3–11 wt%) were loaded in a 50 mL glass bottle sealed by rubber-aluminum cap (Fig. 1c), and heated to 60–100 °C in oil bath for 3–7 h with magnetic stirring. In screening of catalysts and single-factor optimization of the selected catalyst for esterification tests, experiments with one cycled catalyst for each run were conducted directly using the magnetically separated catalyst (Fig. 1d) without ethanol washing. For catalyst cycle tests, the separated catalyst was washed with ethanol for 3 times (or without washing for direct cycle), then dried at 75 °C overnight and named as recovered catalyst for next runs. All experiments were repeated twice and the listed biodiesel yield was average from the two repeated tests with standard deviation (σ) of 0.01–6.24%.

Recovery of catalyst was defined as:

$$\text{Recovery (wt\%)} = (\text{Weight of recovered catalyst}/\text{Weight of fresh catalyst}) \times 100\% \quad (1)$$

For the simultaneous esterification and transesterification of mixed soybean oil with different AVs, mixed soybean oil (0.005 mol), dehydrated methanol and catalyst were loaded, and reacted in a 50 mL micro high-pressure autoclave (YZPR-50, Yanzheng Shanghai Experimental Instrument Co., Ltd.) under the given conditions: oleic acid content (20, 40 and 60 wt%), reaction temperature (120, 140 and 160 °C), reaction time (4, 6 and 8 h, excluding heating time of about 20–30 min), methanol to oil molar ratio of 40/1 and catalyst (7, 9 and 11 wt%) with magnetic stirring (500 rpm) and initial inert N_2 pressure of 3 MPa. The reaction pressure was 5.0–7.0 MPa, which was higher than their corresponding saturated methanol vapor pressures, e.g., 4 MPa at 200 °C to avoid methanol vaporizing to the dead volume of autoclave (about 9.5 mL) [30].

Crude biodiesel was filtered and dried at 75 °C overnight to remove methanol and ethanol (for washing). The treated crude biodiesel including pure FAMEs and oleic acid or soybean oil was analyzed by gas chromatography (GC; GC-2014, Shimadzu, Kyoto) with a capillary column of Rtx-Wax (30 m × Ø0.25 mm × 0.25 μm) under analytical conditions of injector temperature 260 °C, column temperature 220 °C, detector temperature 280 °C, carrier gas (helium) with a flow rate 1 mL/min and split ratio 40/1. FAMEs in crude biodiesel were analyzed using heptadecanoic acid methyl ester (HAME, $C_{17:0}$) as internal standard and relative response factors determined using standard samples of methyl esters, while biodiesel yield (weight percentage of FAMEs in crude biodiesel) was calculated as:

$$\begin{aligned}&\text{Weight of FAMEs in product sample}\\&\quad=(\text{Weight of HAME}\times\text{Chromatographic peak area of methyl esters})/\\&\quad(\text{Chromatographic peak area of HAME}\\&\quad\times\text{Relative response factors for FAMEs})\end{aligned}\tag{2}$$

$$\begin{aligned}\text{Biodiesel yield (wt\%)}&=(\Sigma\ \text{Weight of FAMEs in product sample})/\\&\quad(\text{Weight of crude biodiesel})\times 100\%\end{aligned}\tag{3}$$

Relative response factors for each GC FAMEs were separately calibrated in previous work [28], which were 1.014, 1.023, 1.076, 1.038, 1.019 and 0.926 for palmitate ($C_{16:0}$), linolenate ($C_{16:1}$), stearate ($C_{18:0}$), oleate ($C_{18:1}$), linoleate ($C_{18:2}$) and linolenate ($C_{18:3}$) to that of HAME, respectively.

2.5. Pretreatment of crude *Jatropha* oil

The magnetic solid acid was also used to pretreat crude *Jatropha* oil to reduce AV for further uses (such as transesterification with bases for the production of biodiesel). In a typical esterification of *Jatropha* oil, oil (0.005 mol), dehydrated methanol (methanol to oil molar ratio of 12/1) and catalyst (9 wt%) were loaded in a 50 mL glass bottle sealed by rubber-aluminum cap, and heated to 90 °C in oil bath with magnetic stirring for 1–5 h. After reaction, magnetic catalyst was separated from liquid products by a magnet, and the remained liquid products were filtered for determining the AV. The esterified *Jatropha* oil (0.5–1.0 g) was diluted by 0.25–0.5 g toluene to reduce its viscosity, and titrated by ethanol solution containing KOH with magnetic stirring, using phenolphthalein as indicator. The AV of oil was defined as the weight of consumed KOH divided by the weight of oil based on the standard methods of American Society for Testing and Materials [ASTM, D1980-87 (1998) and D5558-95 (2011)]. The separated catalyst was directly used for next run without ethanol washing for catalyst cycles.

2.6. Regeneration of catalyst

Deactivated catalyst after five cycles from oleic acid esterification was washed with ethanol, filtered and dried at 105 °C. About 5 g of recovered catalyst and 100 mL 98% H_2SO_4 were added into a 150 mL serum bottle, and heated to 150 °C with magnetic stirring for 16 h for regeneration. The sulfonated catalyst was washed with hot water ($\geq$80 °C), filtered and freeze dried. The regenerated catalyst was reused by mixing it (9 wt%) with oleic acid (about 2.82 g) and dehydrated methanol (methanol to oil molar ratio of 12/1) in a glass bottle, and reacted at 90 °C with magnetic stirring for 4 h for oleic acid esterification.

3. Results and discussion

The production of biodiesel experiments were conducted in a sealed glass bottle for esterification (Fig. 1c) and micro autoclave for transesterification. First, the esterification of oleic acid with different carbonaceous magnetic solid acid catalysts was conducted under given conditions to test their magnetism and activity for the selection of catalysts. Secondly, the process optimization of biodiesel production from oleic acid was done with the selected Zr-CMC-SO_3H@3Fe-C_{400} catalyst. Thirdly, the sustainable production of biodiesel (fresh and regenerated catalysts stability experiments for cycles) was carried out under the optimized conditions. Fourthly, the selected catalyst was further applied for producing biodiesel from soybean oil *via* transesterification according to an orthogonal design. Finally, the pretreatment of high AV *Jatropha* oil to reduce AV was investigated with the selected Zr-CMC-SO_3H@3Fe-C_{400} catalyst.

3.1. Oleic acid esterification with synthetic carbonaceous magnetic solid acid catalysts

The esterification experiments with different carbonaceous magnetic solid acid catalysts were conducted under given conditions to test their magnetism and activity for catalyst screening, with results listed in Table 1. Each catalyst was cycled twice after magnetically separated without ethanol washing for the esterification at 90 °C. The results demonstrated that Fe-C_T-SO_3H catalyst calcined at 400, 500 and 600 °C provided poor biodiesel yields of less than 50%, although it could be easily recovered after reactions. The calcination temperatures for Fe-C_T before its sulfonation had great influence on the activity. Low calcination temperatures benefited biodiesel yield. Fe-C_{300}-SO_3H catalyst gave slightly higher biodiesel yield of 50.61%, but showed little magnetism because the chelation of $Fe_2(SO_4)_3$ salt and CMC was not reduced into the magnetic material (Fe_3O_4) at low temperature of 300 °C. Surprisingly, Fe-C_{400} particles even without sulfonation presented considerable activity, with biodiesel yield of 26.53% after esterification for 4 h, which could be due to its weak Lewis acid content from unreduced -COOFe after calcination at 400 °C. After sulfonation with 98% concentrated sulfuric acid at 150 °C for 16 h, the activity of Fe-C_T-SO_3H catalyst didn't improve much because there were not enough functional groups to link sulfuric acid groups on the surface of Fe-C_T particles after high temperature calcination (400–600 °C).

Fe-C_T particles were modified by an additional embedding step using $Fe_2(SO_4)_3$ and CMC solution, and then sulfonated to improve their activity. The prepared Fe-CMC-SO_3H@2Fe-$C_{400/500/600}$ catalysts showed remarkable improvement in biodiesel yield for esterification reaction for 3 h, with yields of 93.12, 87.43 and 93.75% at 400, 500 and 600 °C calcined temperatures for the first catalytic runs and sharply decreased to 74.53, 66.69 and 64.45% for the second recycled runs (Table 1). So, they were not selected due to the instability.

It was found that if Fe-C_T particles were used as magnetic core (e.g., Fe-CMC-SO_3H@2Fe-C_T), the calcination temperature of Fe-C_T played little effect on the activity. Therefore, other commercial magnetic materials such as Fe_3O_4 and Fe particles were directly used instead of Fe-C_T. However, the magnetism of Fe-CMC-SO_3H@nFe_3O_4 and Fe-CMC-SO_3H@nFe catalysts after coated and sulfonated became very weak for separation, because Fe-CMC layer with large pore volume and size that allowed sulfuric acid enter into the magnetic core to dissolve Fe_3O_4 and Fe (Table 1). Therefore, they are not suitable as catalysts.

Fe-C_T particles could be also treated with $ZrOCl_2$ and CMC solutions to produce Zr-CMC-SO_3H@nFe-C_{400} catalyst after sulfonation. The synthesized catalyst of Zr-CMC-SO_3H@2/3Fe-C_{400} both had acceptable magnetism for separation, and showed excellent activity for esterification reaction. After esterification for 3 h with 15/1 methanol/oil ratio and 5 wt% catalyst, biodiesel yield reached 87.59 and 92.93% for the first catalytic run and 73.98 and 86.75% for the second recycled run (Table 1). The increase of Fe-C_{400}

weight from 1 to 3 g in Zr-CMC-SO$_3$H@nFe-C$_{400}$ remarkably increased the recovery rate of catalyst from 81.94 to 99.57%. Zr-CMC-SO$_3$H@3Fe-C$_{400}$ catalyst (with 3 g Fe-C$_{400}$) could be almost recovered after reactions (catalyst recovery rate of 99.57%). Compared with Fe-CMC-SO$_3$H@nFe-C$_T$ catalyst, Zr-CMC as coated layer for Zr-CMC-SO$_3$H@nFe-C$_{400}$ catalyst may have dense surface structure that prevented sulfuric acid from contacting the magnetic core at large extent.

Zr-CMC-SO$_3$H@nFe$_3$O$_4$ and Zr-CMC-SO$_3$H@nFe catalysts with commercial nano- or micro -particles of Fe$_3$O$_4$ and Fe as the magnetic core, gave outstanding activity for oleic acid esterification. Zr-CMC-SO$_3$H@7/5Fe$_3$O$_4$ catalysts gave biodiesel yields of 94.51% and 96.00% for the first catalytic run and 76.72% and 82.44% for the second recycled run, as well as high catalyst recovery of 93.62% and 94.57% after reaction (Table 1). The only concern was that the magnetism of Zr-CMC-SO$_3$H@nFe$_3$O$_4$ catalyst was changeable because Fe$_3$O$_4$ nanoparticles in CMC solution did not mix evenly. Zr-CMC-SO$_3$H@nFe using Fe microparticles as magnetic core, achieved high biodiesel yield of 95.33–98.55% (for Zr-CMC-SO$_3$H@5Fe and Zr-CMC-SO$_3$H@3Fe) for 3 h with methanol/oil molar ratio of 20/1 and catalyst dosage of 5 wt% for the first catalytic run in oleic acid esterification. However, the yield significantly decreased to 62.05–78.28% at the second recycled run. The recovery of catalyst was low when 3 g Fe particles were used as magnetic core, but improved to 92.82–93.55% with the increase of Fe dosage (to 7 and 5 g).

In summary, considering activity, stability and magnetism, Zr-CMC-SO$_3$H@3Fe-C$_{400}$ (Fig. 1b) was selected as a more suitable catalyst for biodiesel production in this work.

3.2. Characterization of Zr-CMC-SO$_3$H@3Fe-C$_{400}$ catalyst

The selected catalyst (Zr-CMC-SO$_3$H@3Fe-C$_{400}$) was characterized by many technologies including XRD, VSM, SEM-EDX, HRTEM, ICP, BET, FT-IR, NaOH titration, elemental analysis and TG-DSC to understand its property, with the results given in Figs. 2–7 and Tables 2 and 3. It had well-crystallized Fe$_3$O$_4$ structures from Fe-C$_{400}$ magnetic core after calcination at 400 °C in Fig. 2. No other peaks were observed for ordered crystalline phases of carbon, suggesting that the carbon structure was amorphous.

The hysteresis loops measurement (Fig. 3) showed that the specific magnetic saturation (Ms) values of Fe-C$_{400}$, fresh and recovered Zr-CMC-SO$_3$H@3Fe-C$_{400}$ catalysts were 6.20, 3.08 and 3.90 Am^2/kg, respectively. The coating of Fe-C$_{400}$ core with Zr-CMC decreased its magnetism, while the removal of coating layer on the outside surface of catalyst during reactions increased the magnetism due to the exposure of magnetic core. The stability of the magnetic strength during cycle can ensure high recovery rate of catalyst for its cycle.

The FT-IR spectrum of Zr-CMC-SO$_3$H@3Fe-C$_{400}$ catalyst (Fig. 4a) had the absorptions for symmetric stretching of COO— at 1629.3 cm^{-1}, for asymmetric stretching of COO— at 1419 cm^{-1} and for symmetric stretching of COO$^-$— at 1743 cm^{-1} due to the formation of —COOFe and —COOZr [31,32]. The stretching of S=O in —SO$_3$H at 1178–1180 cm^{-1} was also found, but the stretching of —SO$_3^-$ at 1026 cm^{-1} and vibration of bidentate —SO$_4^{2-}$ ions at 1218 cm^{-1} were not detected [33].

The acid content over the surface of Zr-CMC-SO$_3$H@3Fe-C$_{400}$ was determined by NaOH titration with value of 8.84 mmol/g, which was higher than other reported catalysts, such as PrSO$_3$H-SBA-15 (0.67 mmol/g), PrSO$_3$H-KIT-6-80/100/120 (0.32/0.25/0.38 mmol/g) [5] and E-260-20-SO$_3$H/E-P400-2-SO$_3$H (5.05/5.35 mmol/g) [34] (Table 2), which was beneficial for esterification under low temperatures.

SEM images (Fig. 5a–i) showed irregular morphology of the fresh solid catalyst with particle size of about 10–100 μm. The particle size and morphology of recovered catalyst changed little

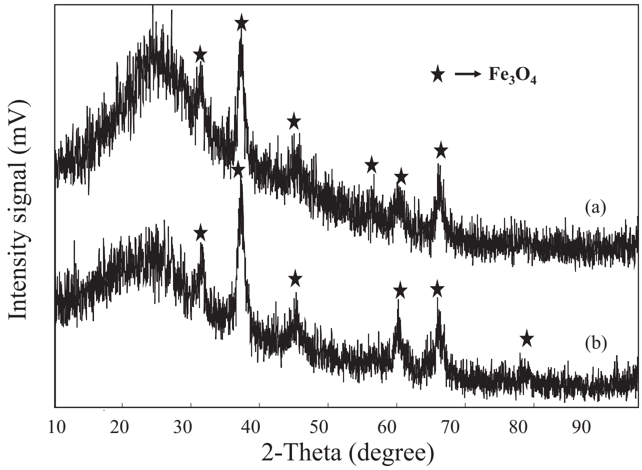

Fig. 2. XRD patterns of (a) Zr-CMC-SO$_3$H@3Fe-C$_{400}$ catalyst and (b) Fe-C$_{400}$ carbonaceous magnetic core.

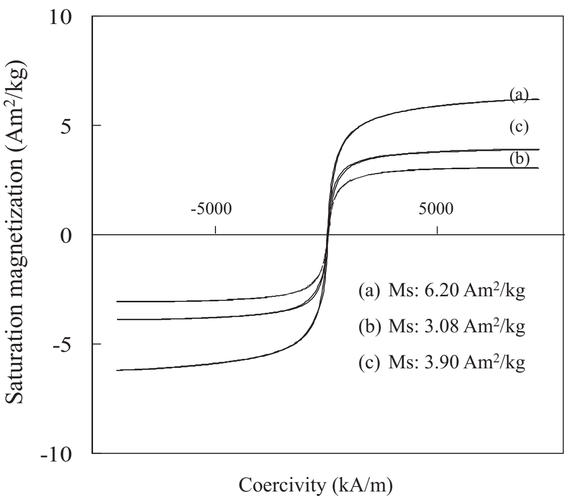

Fig. 3. Hysteresis loops of (a) Fe-C$_{400}$, (b) fresh and (c) recovered catalysts (after one cycle) of Zr-CMC-SO$_3$H@3Fe-C$_{400}$.

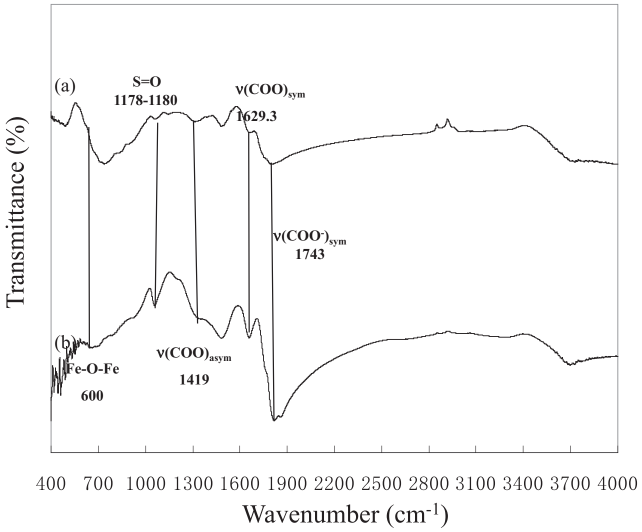

Fig. 4. FT-IR spectra of (a) fresh and (b) regenerated (after five cycles) catalysts of Zr-CMC-SO$_3$H@3Fe-C$_{400}$.

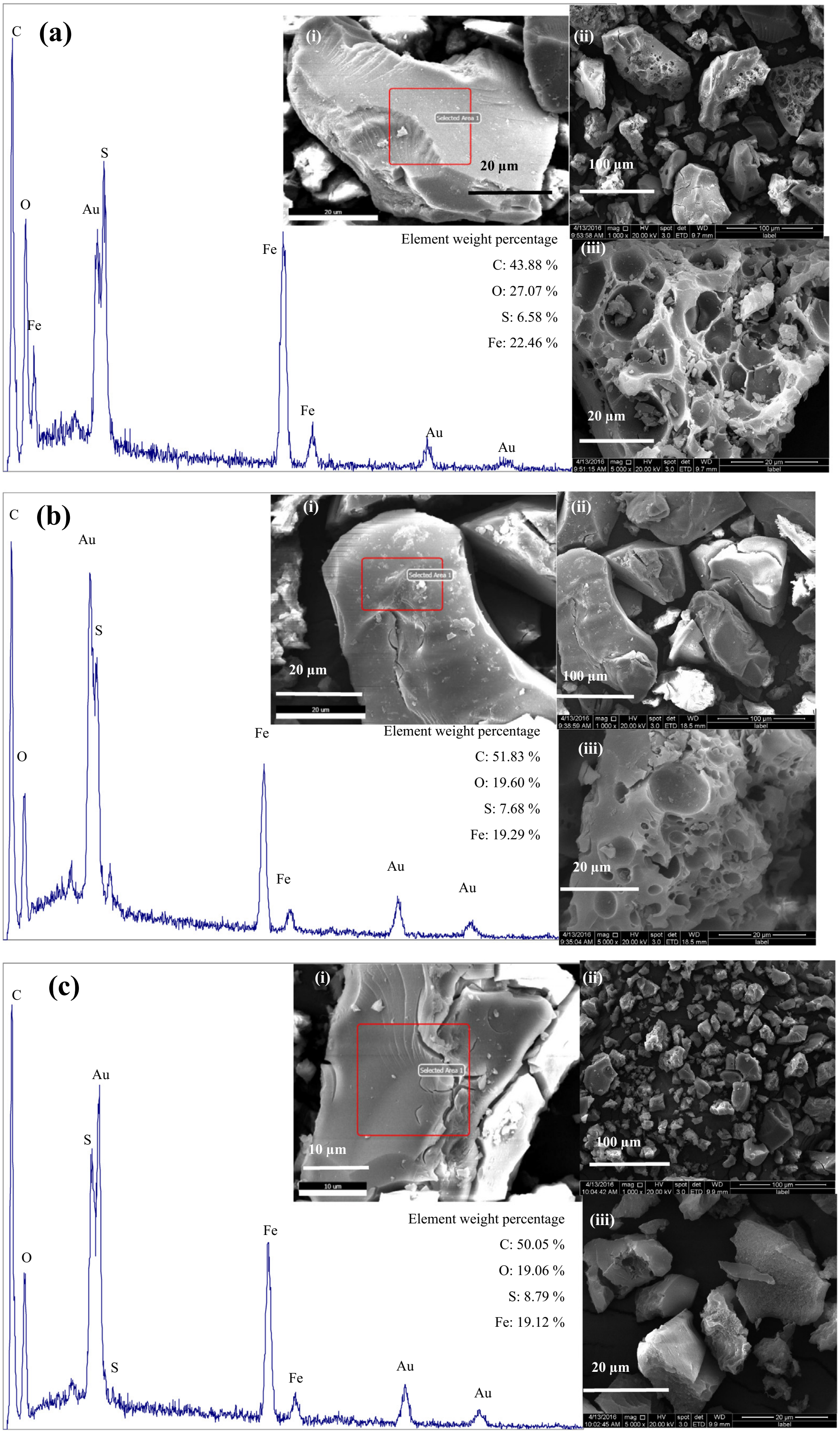

Fig. 5. SEM-EDX spectra and images of (a) fresh, (b) recovered (after 1 cycle), and (c) regenerated (after 5 cycles) catalysts of Zr-CMC-SO_3H@3Fe-C_{400}.

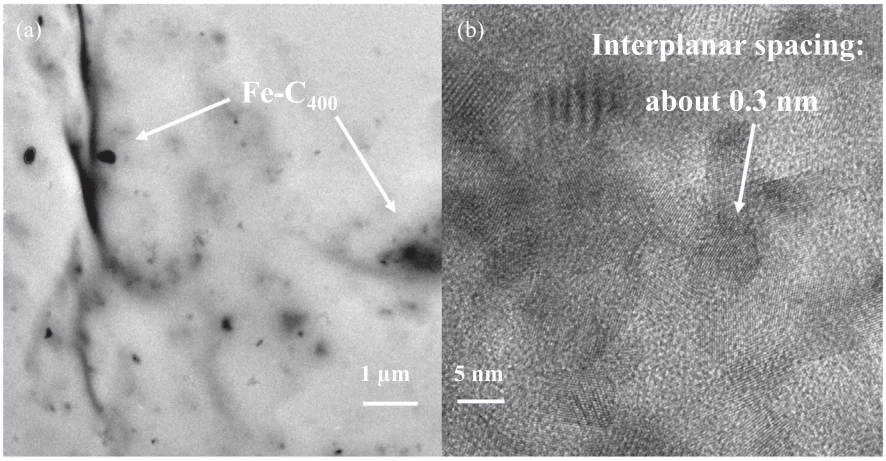

Fig. 6. HRTEM images of fresh Zr-CMC-SO$_3$H@3Fe-C$_{400}$ catalyst.

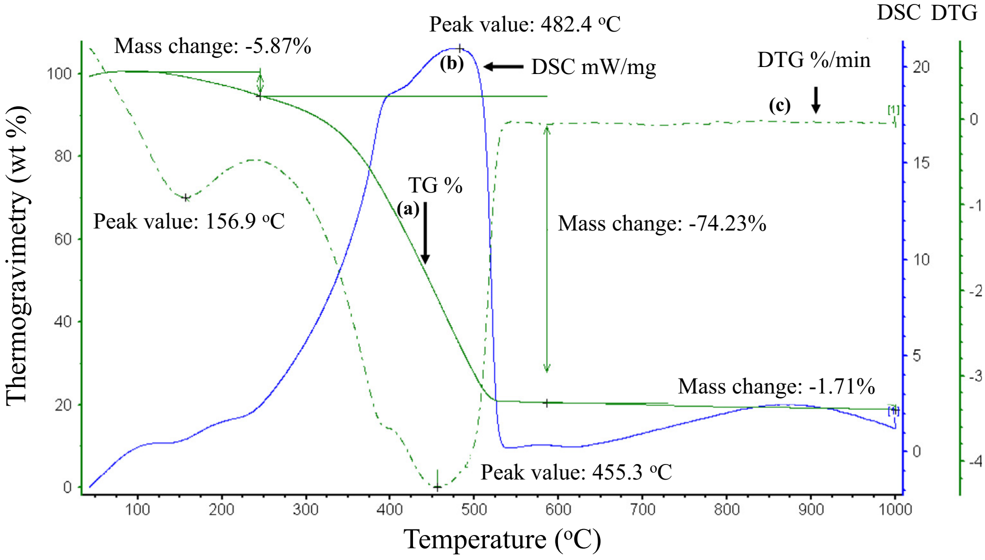

Fig. 7. Thermal stability (TG and DSC) of Zr-CMC-SO$_3$H@3Fe-C$_{400}$ catalyst.

Table 1
The activity and magnetism of catalysts for oleic acid esterification.

	Catalyst magnetism	Catalyst recovery (%)	Biodiesel yield for oleic acid esterification (wt%)	
			For first run	For the second recycled run
Fe-C$_{400}$[a]	Yes	–	26.53 ± 0.99	–
Fe-C$_{300}$-SO$_3$H[b]	No	–	50.61 ± 2.11	–
Fe-C$_{400}$-SO$_3$H[b]	Yes	93.87 ± 3.83	48.31 ± 2.28	–
Fe-C$_{500}$-SO$_3$H[b]	Yes	92.19 ± 1.36	26.36 ± 4.17	–
Fe-C$_{600}$-SO$_3$H[b]	Yes	95.87 ± 4.89	7.80 ± 2.24	–
Fe-CMC-SO$_3$H@nFe$_3$O$_4$, n = 0.5, 1, 1.5, 2, 3, 5, 7 and 9	No	–	–	–
Fe-CMC-SO$_3$H@nFe, n = 5, 7, 9	No	–	–	–
Fe-CMC-SO$_3$H@2Fe-C$_{400}$[b]	Yes	90.64 ± 0.81	93.12 ± 1.30	74.53 ± 4.51
Fe-CMC-SO$_3$H@2Fe-C$_{500}$[b]	Yes	90.81 ± 0.75	87.43 ± 1.34	66.69 ± 2.50
Fe-CMC-SO$_3$H@2Fe-C$_{600}$[b]	Yes	94.75 ± 0.81	93.75 ± 1.08	64.45 ± 6.24
Zr-CMC-SO$_3$H@5Fe$_3$O$_4$[b]	Yes, but unstable	94.57 ± 0.76	96.00 ± 0.27	82.44 ± 0.29
Zr-CMC-SO$_3$H@7Fe$_3$O$_4$[b]	Yes, but unstable	93.62 ± 0.79	94.51 ± 0.39	76.72 ± 0.18
Zr-CMC-SO$_3$H@9Fe$_3$O$_4$[b]	Yes, but unstable	99.08 ± 1.30	94.68 ± 0.32	80.55 ± 0.10
Zr-CMC-SO$_3$H@3Fe[b]	Yes	57.08 ± 1.30	98.55 ± 0.26	78.28 ± 0.45
Zr-CMC-SO$_3$H@5Fe[b]	Yes	93.55 ± 0.64	95.33 ± 0.11	67.51 ± 0.78
Zr-CMC-SO$_3$H@7Fe[b]	Yes	92.82 ± 0.49	97.72 ± 0.49	62.05 ± 1.95
Zr-CMC-SO$_3$H@1Fe-C$_{400}$[c]	Yes	81.94 ± 0.54	90.07 ± 0.04	78.98 ± 0.11
Zr-CMC-SO$_3$H@2Fe-C$_{400}$[c]	Yes	89.61 ± 0.59	87.59 ± 3.42	73.98 ± 0.41
Zr-CMC-SO$_3$H@3Fe-C$_{400}$[c]	Yes	99.57 ± 0.62	92.93 ± 2.43	86.75 ± 0.74

[a] Conditions: 90 °C, 4 h, methanol/oil molar ratio of 12/1, catalyst dosage of 9 wt%.
[b] Conditions: 90 °C, 3 h, methanol/oil molar ratio of 20/1, catalyst dosage of 5 wt%.
[c] Conditions: 90 °C, 3 h, methanol/oil molar ratio of 15/1, catalyst dosage of 5 wt%.

Table 2
Comparison of the acidity and specific magnetic saturation (Ms) of Zr-CMC-SO_3H@3Fe-C_{400} in this work with previous studies.

Catalysts	Magnetism (Ms: Am^2/kg)	Biodiesel yield	Acid content (mmol/g)		Ref.
		Esterification	NaOH titration	TPD	
Zr-CMC-SO_3H@3Fe-C_{400}					This study
Fresh	3.08	99.57% for 4.0 h	8.84	–	
Recovered after first cycle[a]	3.90		6.56	–	
Regenerated	–	93.97% for 4.0 h	8.62	–	
After five cycles[a] of regenerated catalyst	–		7.22	–	
Amberlyst-15	0.0	45.00% for 6.0 h	–		[5]
$PrSO_3H$-SBA-15	0.0	35.60% for 6.0 h	0.67		[5]
$PrSO_3H$-KIT-6-80	0.0	13.60% for 6.0 h	0.32		[5]
$PrSO_3H$-KIT-6-100	0.0	27.60% for 6.0 h	0.25		[5]
$PrSO_3H$-KIT-6-120	0.0	39.30% for 6.0 h	0.38		[5]
E-260-20-SO_3H	0.0	95.40% for 7.0 h	5.05	–	[34]
E-P400-2-SO_3H	0.0	95.50% for 5.0 h	5.35	–	[34]

[a] Conditions for oleic acid esterification: 90 °C, 4 h, methanol/oil molar ratio of 12/1, catalyst dosage of 9 wt%, without ethanol washing for each cycle.

Table 3
Elemental compositions (N, C, H, S, Fe and Zr) of catalyst analyzed by organic elemental analyzer and ICP.

Catalysts	Elemental composition by ICP and organic elemental analysis (wt%)						Atomic ratio	
	N	C	H	S	Fe	Zr	S/C	Fe/C
Fe-C_{400}	–[b]	–[b]	–[b]	–[b]	13.07	–[b]		
Zr-CMC-SO_3H@3Fe-C_{400},								
Fresh	0.03	49.55	2.93	3.60	5.76	0.36	0.027[c], 0.056[d]	0.087[c], 0.384[d]
Recovered after first cycle[a]	0.03	53.2	3.14	3.27	7.86	–	0.023[c], 0.056[d]	0.111[c], 0.279[d]
Recovered after five cycles[a]	0.02	60.70	4.80	1.74	–	0.35	0.011[c]	–[c]
Regenerated	0.10	54.05	2.93	3.66	–	–	0.025[c], 0.066[d]	–[c], 0.287[d]
After five cycles[a] of regenerated catalyst	0.13	57.64	3.54	2.90	–	–	0.019[c]	–[c]

[a] Conditions for oleic acid esterification: 90 °C, 4 h, methanol/oil molar ratio of 12/1, catalyst dosage of 9 wt%, without ethanol washing for each cycle.
[b] The determination was not performed.
[c] Elemental ratio in bulk phase determined by ICP and organic elemental analysis.
[d] Elemental ratio in surface phase determined by EDX.

as compared with the fresh one (Fig. 5 b *vs.* a ii and iii). But, the particle size after regenerated from the deactivated five cycled catalyst significantly decreased, and the particle surface became smoother as compared with the fresh one (Fig. 5 c *vs.* a ii and iii) due to the mechanical crushing.

HRTEM image (Fig. 6a) showed the Fe-C_{400} magnetic core particles were evenly spread in the carbon-based carrier of the fresh catalyst. Slight agglomeration of the magnetic particles was observed due to their attraction each other. In Fig. 6b, the overlapping crystal grains attracted by magnetic force with inter planar spacing of about 0.3 nm were found. Based on the XRD result in Fig. 2, it was presumed that the crystal grains were Fe_3O_4 nanoparticles.

The BET surface area of the fresh catalyst was 8.02 m^2/g, with average pore size of about 32.3 nm, which benefited the access of oleic acid and methanol molecules as the size of free fatty acids and methanol was less than 4 nm [35].

EDX (C, O, S and Fe), ICP (Zr and Fe) and organic elemental analysis (C, H, N and S) (Table 3) showed the difference of elemental compositions between the surface and bulk of Zr-CMC-SO_3H@3Fe-C_{400} catalyst. The fresh catalyst contained 3.60% S and 49.55% C from elemental analysis, and 5.76% Fe but only 0.36% Zr by ICP. It demonstrated that most of Zr might be dissolved during sulfonation of Zr-CMC@3Fe-C_{400}, and no Zr was detected on the surface of catalyst by EDX. The atomic ratios of S/C and Fe/C on the surface of the fresh catalyst (0.056 and 0.384, respectively by EDX) were higher than those in the bulk catalyst (0.027 and 0.087 by elemental analysis and ICP), demonstrating that Fe and sulfonic groups were enriched over the catalyst surface. The recovered catalyst after one catalytic run had higher C content in bulk, which was attributed to the possible adsorption of reaction by-products such as glycerol in the catalyst pores, while the decline of O and Fe contents over catalyst surface (by EDX) suggested the possible leaching of —COOFe groups during the reactions. The S content over catalyst surface showed no remarkable decrease after the first run.

TG-DSC curves (Fig. 7a) showed that the catalyst was mainly decomposed at 250–580 °C, accompanied by weight loss of 74.23 wt% with remarkable exothermic behavior (Fig. 7b), which was attributed to the decomposition of —COOZr and —COOFe structures and the release of various oxygen-containing groups. However, Zr-CMC-SO_3H@3Fe-C_{400} was quite stable below 200 °C region that was for biodiesel production.

3.3. Single-factor experiments of oleic acid esterification

The optimization of biodiesel production by single-factor experiments was done with the selected catalyst Zr-CMC-SO_3H@3Fe-C_{400}. The influence of reaction conditions including temperature, time, methanol/oil molar ratio and catalyst dosage was studied for the esterification of oleic acid in Fig. 8. The recycled catalyst after the first run without ethanol washing was also tested to see its stability.

The effect of reaction temperature was studied under reaction time of 3 h, methanol/oil ratio of 15/1 and catalyst of 5 wt% (Fig. 8A). Biodiesel yield varied from 82.69% to 92.93% with

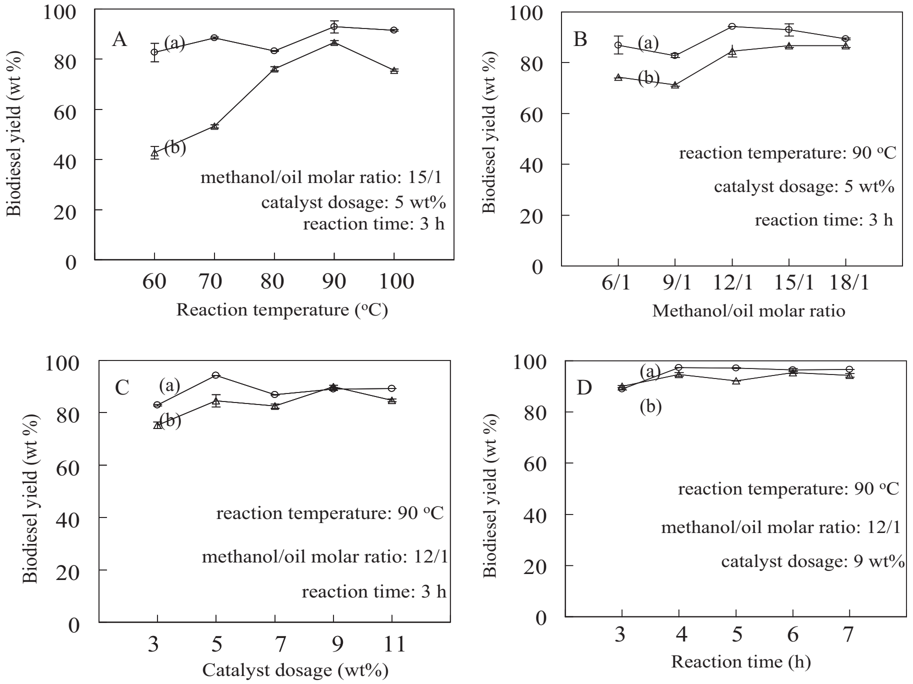

Fig. 8. Single-factor experiments of oleic acid esterification with (a) fresh Zr-CMC-SO_3H@3Fe-C_{400} catalyst and (b) recycled catalyst from the first run without washing: (A) reaction temperature, (B) methanol/oil molar ratio, (C) catalyst dosage and (D) reaction time.

temperature increased from 60 to 90 °C. Temperature had remarkable effect on the yield of biodiesel over the recovered catalyst. Biodiesel yield increased sharply from 42.72% to the maximum value of 86.75% as temperature rose from 60 to 90 °C and dropped to 75.63% when temperature further increased to 100 °C. The deactivation of catalyst came from the loss of active sites at high temperature and the coverage of active sites by by-products such as glycerol as the catalyst was not washed after reactions. So, temperature of 90 °C was selected for the following experiments.

The effect of methanol/oil molar ratio was studied at 90 °C, 3 h and 5 wt% catalyst (Fig. 8B). Biodiesel yield first increased and declined as methanol/oil ratio increased from 9/1 to 18/1, and gave the maximum yield of 94.25% for the first run and 84.52% for the second recycled run at methanol/oil ratio of 12/1. Excess methanol/oil ratio was not beneficial for oleic acid esterification because it significantly decreased the concentration of catalyst in the reaction mixture [36]. So, methanol/oil ratio of 12/1 was selected for the following experiments.

The impact of catalyst dosage was studied at 90 °C, 3 h and 12/1 methanol/oil ratio (Fig. 8C). Increasing catalyst weight in the reaction mixture might improve the contact of reactants with catalyst surface, but possibly affected the mass transfer during reactions. Therefore, biodiesel yield over the fresh catalyst achieved its maximum value of 94.25% at 5 wt% catalyst (84.52% for recovered catalyst). But, biodiesel yield over fresh and the recovered catalyst were 88.97% and 89.98% at 9 wt% catalyst, and thus catalyst dosage of 9 wt% was selected for the study on the effect of reaction time.

In Fig. 8D, biodiesel yield with the fresh catalyst grew from 88.97% to 97.39% when time prolonged from 3 to 4 h and decreased slightly to 96.60% at 7 h, while the recovered catalyst showed similar trend with reaction time. So, time of 4 h was selected for subsequent experiments.

In conclusion, the best conditions with biodiesel yield of 97.39% for oleic acid esterification with Zr-CMC-SO_3H@3Fe-C_{400} catalyst were reaction temperature of 90 °C, methanol/oil molar ratio of 12/1, 9 wt% catalyst and reaction time of 4 h. These conditions were used in the following sustainable production of biodiesel with recovered and regenerated catalysts.

3.4. Sustainable production of biodiesel with recovered and regenerated catalysts

The sustainable production of biodiesel was studied under the best conditions (90 °C for 4 h, with methanol/oil molar ratio of 12/1 and catalyst dosage of 9 wt%) optimized by single-factor experiments with selected Zr-CMC-SO_3H@3Fe-C_{400} catalyst. The catalyst was recovered from products after reaction with or without ethanol washing after each cycle to reuse for the sustainable biodiesel production. Biodiesel yield after five cycles decreased from 97.39% to 86.87% for the cycled catalyst without ethanol washing, and from 97.39% to 79.56% for the washed catalyst after each cycle. It seemed that ethanol washing was a dispensable step for the post-treatment of solid catalyst after separation. The recovery of the catalyst with ethanol washing was 91.98%, and 89.99% without washing after the fifth cycle (Fig. 9).

The deactivated catalyst after five cycles without ethanol washing for each run was sulfonated again using concentrated sulfuric acid for regeneration, and the activity of the regenerated catalyst was tested using oleic acid esterification reaction (Fig. 10). Biodiesel yield slightly decreased from 93.97% to 90.16% with the regenerated catalyst at the fifth cycle. The recovery rate of solid catalyst after five cycles of the regenerated catalyst was 90.46%, which was slight higher than that of fresh catalyst (89.99%).

SEM, FT-IR, NaOH titration and elemental analysis were also performed for the characterization of recovered and regenerated catalysts (Figs. 4 and 5 and Tables 2 and 3). The regenerated catalyst showed significantly smaller particle size of about 5–20 μm than 10–100 μm for the fresh catalyst (Fig. 5c). After the regeneration, the deactivated catalyst recovered most of the surface acid content and S content (Tables 2 and 3). The S/C atomic ratio in the regenerated catalyst (0.066) was even higher than that of the fresh catalyst (0.056), accompanied by stronger IR absorptions of COO^- stretching, COO stretching and S=O stretching (for $-SO_3H$ groups) (Fig. 4). The sulfonic acid group in the regenerated catalyst (S content of 3.66% and 2.90% for fresh and recovered one after five cycles) seemed more stable than that in the fresh catalyst (S content of 3.60% and 1.74% for fresh and recovered catalyst after five

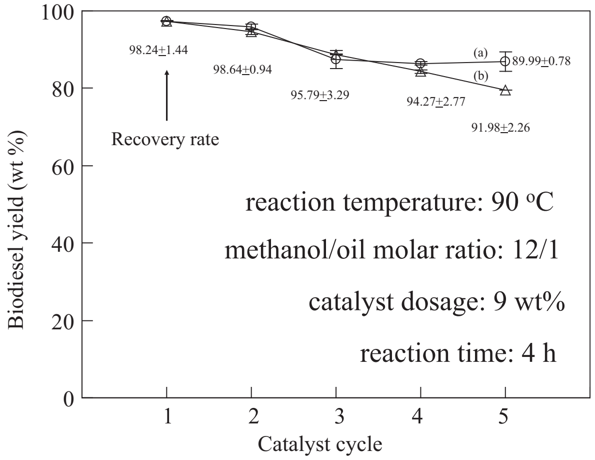

Fig. 9. Oleic acid esterification with (a) the recycled Zr-CMC-SO_3H@3Fe-C_{400} catalyst without washing and (b) washed with ethanol after each cycle.

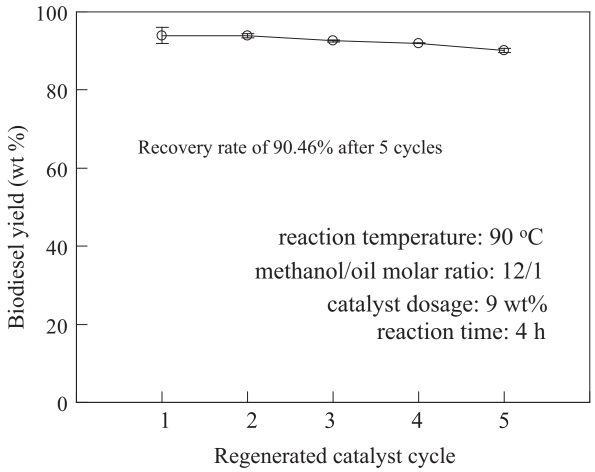

Fig. 10. Oleic acid esterification with regenerated Zr-CMC-SO_3H@3Fe-C_{400} catalyst after five cycles.

cycles), which was possibly due to the removal of unbonded carbon on catalyst surface during the esterification reaction and second sulfonation. After five cycles for the regenerated catalyst, the surface acid content and the S content in bulk phase just decreased from 8.62 to 7.22 mmol/g, and from 3.66% to 2.90%, respectively.

3.5. Production of biodiesel from soybean oil

Since biodiesel was mainly produced by transesterification of triglycerides in plan oils or animal fats. Therefore, commercial soybean oil was blended with 20, 40 and 60 wt% oleic acid to simulate other high AV oils. The selected catalyst was used to catalyze the mixed soybean oil with high AV by the simultaneous transesterification and esterification reaction to biodiesel. An orthogonal deign with four factors at three levels (oleic acid content of 20, 40 and 60 wt%, temperature of 120, 140 and 160 °C, catalyst dosage of 7, 9 and 11 wt% and reaction time of 4, 6 and 8 h) was designed for experiments (Table 4). In Table 4, parameter K had the order of $K_3 > K_2 > K_1$ for oleic acid content, $K_2 > K_1 > K_3$ for reaction temperature, $K_2 > K_3 > K_1$ for catalyst dosage and $K_3 > K_2 > K_1$ for reaction time. Therefore, the optimized conditions for the reaction of mixed soybean oil over Zr-CMC-SO_3H@3Fe-C_{400} catalyst were oleic acid content of 60 wt%, reaction temperature of 140 °C, catalyst dosage of 9 wt% and reaction time of 8 h, with the optimized biodiesel yield of 95.40%. According to the range analysis, the influence of four factors on biodiesel yield followed the order: oleic acid content (extreme value R = 3.340) > catalyst dosage (1.561) > reaction temperature (1.047) > reaction time (0.790).

3.6. Pretreatment of high AV *Jatropha* oil

Jatropha oil with high AV was pretreated with Zr-CMC-SO_3H@3Fe-C_{400} catalyst. *Jatropha* oil with AV of 17.2 mg KOH/g, dehydrated methanol (methanol/oil ratio of 12/1) and catalyst (9 wt%) were loaded in a 50 mL glass bottle sealed by rubber-aluminum cap, and reacted at 90 °C in oil bath with magnetic stirring for 1–5 h. The results were plotted in Fig. 11. The AV of *Jatropha* oil decreased to 3.81 mg KOH/g after reaction with the fresh catalyst for 1 h, and further decreased to 0.71 mg KOH/g after 3 h. But for the second recovered catalyst, it needed 4 h to decrease AV to lower than 0.7 mg KOH/g. So, the proper time for the pretreatment of high AV *Jatropha* oil was 4 h. Catalyst cycle was also tested (Fig. 11B), however, the AV of *Jatropha* oil significantly increased to higher than 1 mg KOH/g after the second cycle. It demonstrated that the activity and stability of Zr-CMC-SO_3H@3Fe-C_{400} still needed improvement for the pre-esterification of high AV oils.

3.7. Industrial applications

Nowadays, biodiesel has been applied for the supplement of fossil diesel to reduce the dependent on imported oil and environmental pollution. The European Parliament and Canadian government established energy strategy to answer the growing shortage

Table 4
Orthogonal experimental design $L_9(4)^5$ and results for the reaction of mixed soybean oils over fresh Zr-CMC-SO_3H@3Fe-C_{400} catalyst.

No.	A	B	C	D	Biodiesel yield (wt%)
	Weight content of oleic acid (wt%)	Temperature (°C)	Catalyst dosage (wt%)	Reaction time (h)	
1	20	120	7	4	88.90 ± 2.06
2	20	140	9	6	90.72 ± 1.96
3	20	160	11	8	89.15 ± 0.08
4	40	120	9	8	92.99 ± 1.65
5	40	140	11	4	91.19 ± 0.11
6	40	160	7	6	89.94 ± 0.12
7	60	120	11	6	92.97 ± 0.23
8	60	140	7	8	93.07 ± 0.13
9	60	160	9	4	92.75 ± 0.52
K_1	89.590	91.620	90.637	90.947	
K_2	91.373	91.660	92.153	91.210	
K_3	92.930	90.613	91.103	91.737	
R_1	3.340	1.047	1.516	0.790	

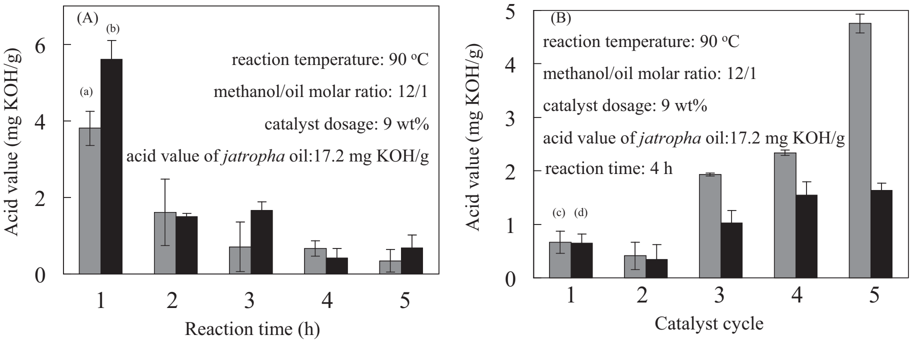

Fig. 11. Pretreatment (esterification) of *Jatropha* oil with (a) fresh, (b) recovered Zr-CMC-SO_3H@3Fe-C_{400} catalyst after one cycle, (c) recycled Zr-CMC-SO_3H@3Fe-C_{400} catalyst with ethanol washing and (d) without washing after each cycle.

of resources [2,37]. But biodiesel industrial production is still underdeveloped especially in developing countries due to high total cost from raw oils and production process. The expense from raw oils is 70–95% of total cost if edible oils (including vegetable oils and animal fat) are used [38]. Hence, exploiting non-edible oils with inexpensive price is very important for developing countries to reduce the total cost [1,39] with only 24–32% cost in raw oils [40]. Zhang et al reported base catalyzed transesterification was a cost-effective way with soybean or rapeseed oil as raw oils, yet acid catalysis could reduce the total cost by 27% when high AV oils were used [40]. *Jatropha* oil as non-edible oil from *Jatropha* curcas L. (belonging to the Euphorbiaceae family) [41] trees having strong drought resistance and growing in abandoned and fallow farmlands [1] is considered as ideal raw oil for the synthesis of biodiesel, with market value of between 350 and 500 US$/ton [42]. Industrial production of *Jatropha* biodiesel and pretreatment are usually catalyzed by sulfuric acid and NaOH for its cheap price and good catalytic ability on the esterification and transesterification reactions, for example for Yunnan Shenyu New Energy Co., Ltd in China. It was reported that only with 1 wt% sulfuric acid (95.4% concentration), under conditions of temperature of 120 °C for > 20 h and methanol/soybean oil molar ratio of 9/1, FAMEs yield could reach > 99% [43]. But, high temperatures and corrosion-resistant equipment are required if liquid sulfuric acid was only used as catalyst. Moreover, it is difficult to recover the acid and usually requires the neutralization step which produces a large amount of wastewater to cause environmental pollution. In order to promote the sustainable energy development and reduce the cost of biodiesel production, efficient and easy separated solid catalysts need to be developed. In this work, the sustainable production of biodiesel catalyzed by synthesized magnetic Zr-CMC-SO_3H@3Fe-C_{400} solid acid catalyst could be realized due to its recyclability with >ten cycles (> 90% biodiesel yield from esterification), high catalytic activity in transesterification (FAMEs yield > 95% from soybean oil), moderate magnetism (3.08 Am^2/kg) and environmental friendliness (without wastewater disposal) which could reduce the cost of biodiesel production, the energy consumption of products separation, avoid wastewater discharge and extend equipment life. So, this work provided more choices for the commercial biodiesel production.

4. Conclusions

Biodiesel production via esterification or transesterification reaction can be successfully catalyzed by the synthesized magnetic Zr-CMC-SO_3H@3Fe-C_{400} catalyst. The catalyst was active to produce biodiesel by esterification with maximum yield of 97.39% at 90 °C and was easily separated by a magnet for ten cycles (biodiesel yield > 90%) if regeneration step was applied. For transesterification reaction, biodiesel yield could reach 95.40% from high AV oils. Catalyst had very high activity on pretreatment of high AV Jatropha oil with five cycles (AV reduced to 1.64 mg KOH/g).

Acknowledgements

The authors wish to acknowledge the financial support from Nanjing Agricultural University (No. 68Q-0603).

References

[1] Atabani AE, Silitonga AS, Ong HC, Mahlia TMI, Masjuki HH, Badruddin Irfan Anjum, et al. Non-edible vegetable oils: a critical evaluation of oil extraction, fatty acid compositions, biodiesel production, characteristics, engine performance and emissions production.. Renew Sust Energ Rev 2013;18:211–45.
[2] Guo M, Littlewood J, Joyce J, Murphy R. The environmental profile of bioethanol produced from current and potential future poplar feedstocks in the EU. Green Chem 2014;16:4680–95.
[3] Roy MM, Wang W, Bujold J. Biodiesel production and comparison of emissions of a DI diesel engine fueled by biodiesel–diesel and canola oil–diesel blends at high idling operations. Appl Energy 2013;106:198–208.
[4] Moore RH, Thornhill KL, Weinzierl B, Sauer D, Ascoli ED, Kim J, et al. Biofuel blending reduces particle emissions from aircraft engines at cruise conditions. Nature 2017;543:411–5.
[5] Pirez C, Caderon JM, Dacquin JP, Lee AF, Wilson K. Tunable KIT-6 mesoporous sulfonic acid catalysts for fatty acid esterification. ACS Catal 2012;2:1607–14.
[6] Sankaranarayanan S, Antonyraj CA, Kannan S. Transesterification of edible, non-edible and used cooking oils for biodiesel production using calcined layered double hydroxides as reusable base catalysts. Bioresour Technol 2012;109:57–62.
[7] Jacobson MZ. Review of solutions to global warming, air pollution, and energy security. Energy Environ Sci 2009;2:148–73.
[8] Ragauskas AJ, Williams CK, Davison BH, Britovsek G, Cairney J, Eckert CA, et al. The path forward for biofuels and biomaterials. Science 2006;311:484–9.
[9] Al-Sakkari EG, El-Sheltawy ST, Attia NK, Mostafa SR. Kinetic study of soybean oil methanolysis using cement kiln dust as a heterogeneous catalyst for biodiesel production. Appl Catal B-Environ 2017;206:146–57.
[10] Corro G, Pal U, Tellez N. Biodiesel production from Jatropha curcas crude oil using ZnO/SiO2 photocatalyst for free fatty acids esterification. Appl Catal B-Environ 2013;129:39–47.
[11] Torregrosa AJ, Broatch A, Pla′ B, Mónico LF. Impact of FischereTropsch and biodiesel fuels on trade-offs between pollutant emissions and combustion noise in diesel engines. Biomass Bioenergy 2013;52:22–33.
[12] USEPA. A comprehensive analysis of biodiesel impacts on exhaust emissions. EPA420-P-02-001; 2002.
[13] Senatore A, Cardone M, Buono D. Combustion study of a common rail diesel engine optimized to be fueled with biodiesel. Energy Fuel 2008;22:1405–10.
[14] Muncrief RL, Rooks CW, Cruz M, Harold MP. Combining biodiesel and exhaust gas recirculation for reduction in NOx and particulate emissions. Energy Fuel 2008;22:1285–96.
[15] Thompson GJ, Nuszkowski J. Neat fuel influence on biodiesel blend emissions. Int J Engine Res 2010;11:61–77.
[16] Bunce M, Snyder D, Adi G, Hall C, Koehler J, Davila B, et al. Stock and optimized performance and emissions with 5 and 20% soy biodiesel blends in a modern common rail turbodiesel engine. Energy Fuel 2010;24:928–39.
[17] Qiu F, Li Y, Yang D, Li X, Sun P. Biodiesel production from mixed soybean oil and rapeseed oil. Appl Energy 2011;88:2050–5.
[18] Saravanan S, Nagarajan G, Lakshmi Narayana Rao G, Sampath S. Theoretical and experimental investigation on effect of injection timing on NOx emission of biodiesel blend. Energy 2014;66:216–21.

[19] Nabi M, Rahman M, Akhter S. Biodiesel from cotton seed oil and its effect on engine performance and exhaust emissions. Appl Therm Eng 2009;29:2265–70.

[20] Martín M, Grossmann IE. Design of an optimal process for enhanced production of bioethanol and biodiesel from algae oil via glycerol fermentation. Appl Energy 2014;135:108–14.

[21] Long YD, Fang Z, Su TC. Co-production of biodiesel and hydrogen from rapeseed and *Jatropha* oils with sodium silicate and Ni catalysts. Appl Energy 2014;113:1819–25.

[22] Karatay SE, Dönmez G. Microbial oil production from thermophile cyanobacteria for biodiesel production. Appl Energy 2011;88:3632–5.

[23] Creasey JJ, Parlett CMA, Manayil JC, Isaacs MA, Wilson K, Lee AF. Facile route to conformal hydrotalcite coatings over complex architectures: a hierarchically ordered nanoporous base catalyst for FAME production. Green Chem 2015;17:2398–405.

[24] Pua FL, Fang Z, Zakaria S, Chia CH, Guo F. Direct production of biodiesel from high-acid value *Jatropha* oil with solid acid catalyst derived from lignin.. Biotechnol Biofuels 2011;4:56.

[25] Mazzotta MG, Gupta D, Saha B, Patra AK, Bhaumik A, Abu-Omar MM. Efficient solid acid catalyst containing Lewis and Brønsted acid sites for the production of furfurals. ChemSusChem 2014;7:2342–50.

[26] Zhang Y, Wong WT, Yung KF. Biodiesel production via esterification of oleic acid catalyzed by chlorosulfonic acid modified zirconia. Appl Energy 2014;116:191–8.

[27] Thanasilp S, Schwank JW, Meeyoo V, Pengpanich S, Hunsom M. One-pot oxydehydration of glycerol to value-added compounds over metal-doped SiW/HZSM-5 catalysts: Effect of metal type and loading. Chem Eng J 2015;275:113–24.

[28] Xue BJ, Luo J, Zhang F, Fang Z. Biodiesel production from soybean and *Jatropha* oils by magnetic $CaFe_2O_4$-$Ca_2Fe_2O_5$-based catalyst. Energy 2014;68:584–91.

[29] Boehm HP. Surface oxides on carbon and their analysis: a critical assessment. Carbon 2002;40:145–9.

[30] Wang YT, Fang Z, Zhang F, Xue BJ. One-step production of biodiesel from oils with high acid value by activated Mg–Al hydrotalcite nanoparticles. Bioresour Technol 2015;193:84–9.

[31] Boey PL, Ganesan S, Maniam GP, Khairuddean M, Lee SE. A new heterogeneous acid catalyst system for esterification of free fatty acids into methyl esters. Appl Catal A-Gen 2012;433–434:12–7.

[32] Wang J, Lin XY, Luo XG, Long YF. A sorbent of carboxymethyl cellulose loaded with zirconium for the removal of fluoride from aqueous solution. Chem Eng J 2014;252:415–22.

[33] Yadav GD, Murkute AD. Preparation of a novel catalyst UDCaT-5: enhancement in activity of acid-treated zirconia—effect of treatment with chlorosulfonic acid vis-à-vis sulfuric acid. J Catal 2004;224:218–23.

[34] Huang M, Luo J, Fang Z, Li H. Biodiesel production catalyzed by highly acidic carbonaceous catalystssynthesized via carbonizing lignin in sub- and super-critical ethanol. Appl Catal B-Environ 2016;190:103–14.

[35] Geng L, Yu G, Wang Y, Zhu YX. Ph-SO_3H-modified mesoporous carbon as an efficient catalyst for the esterification of oleic acid. Appl Catal A-Gen 2012;427–428:137–44.

[36] Zhang F, Fang Z, Wang YT. Biodiesel production direct from high acid value oil with a novel magnetic carbonaceous acid. Appl Energy 2015;155:637–47.

[37] Directive 2009/28/EC. On the promotion of the use of energy from renewable sources and amending and subsequently repealing directives 2001/77/EC and 2003/30/EC. OJEU 2009;L 140:16–62.

[38] Connemann J, Fischer J. Biodiesel in Europe 1998: biodiesel processing technologies. In: Paper presented at the international liquid biofuels congress, Brazil [15 pp.].

[39] Živković SB, Veljković MV, Banković-Ilić IB, Krstić IM, Konstantinović SS, Ilić SB, et al. Technological, technical, economic, environmental, social, human health risk, toxicological and policy considerations of biodiesel production and use. Renew Sust Energ Rev 2017;79:222–47.

[40] Zhang Y, Dube MA, McLean DD, Kates M. Biodiesel production from waste cooking oil: 2. Economic assessment and sensitivity analysis. Bioresour Technol 2003;90:229–40.

[41] Kibazohi O, Sangwan RS. Vegetable oil production potential from Jatropha curcas, Croton megalocarpus, Aleurites moluccana, Moringa oleifera and Pachira glabra: assessment of renewable energy resources for bio-energy production in Africa. Biomass Bioenergy 2011;35:1352–6.

[42] Lee RA, Lavoie J. From first– to third–generation biofuels: challenges of producing a commodity from a biomass of increasing complexity. Anim Front 2013;3:6–11.

[43] Goff MJ, Bauer NS, Lopes S, Sutterlin WR, Suppes GJ. Acid-catalyzed alcoholysis of soybean oil. J Am Oil Chem Soc 2004;81:415–20.